We are IntechOpen,
the world's leading publisher of
Open Access books
Built by scientists, for scientists

4,800
Open access books available

122,000
International authors and editors

135M
Downloads

Our authors are among the

154
Countries delivered to

TOP 1%
most cited scientists

12.2%
Contributors from top 500 universities

CLARIVATE ANALYTICS
BOOK CITATION INDEX
INDEXED

WEB OF SCIENCE™

Selection of our books indexed in the Book Citation Index
in Web of Science™ Core Collection (BKCI)

Interested in publishing with us?
Contact book.department@intechopen.com

Numbers displayed above are based on latest data collected.
For more information visit www.intechopen.com

Design Issues in Radio Frequency Energy Harvesting System

Chomora Mikeka and Hiroyuki Arai
Yokohama National University
Japan

1. Introduction

Emerging self powered systems challenge and dictate the direction of research in energy harvesting (EH). State of the art in energy harvesting is being applied in various fields using different single energy sources or a combination of two or more sources. In certain applications like smart packaging, radio frequency (RF) is the preferred method to power the electronics while for smart building applications, the main type of energy source used is solar, with vibration & thermal being used increasingly. The main differences in these power sources is the power density; for example RF ($0.01 \sim 0.1$ μW/cm^2), Vibration ($4 \sim 100$ μW/cm^2), Photovoltaic (10 μW/cm$^2 \sim 10$mW/cm^2) and Thermal (20 μW/cm$^2 \sim 10$mW/cm^2). Obviously RF energy though principally abundant, is the most limited source on account of the incident power density metric, except when near the base stations. Therefore, in general, RF harvesting circuits must be designed to operate at the most optimal efficiencies.

This Chapter focuses on RF energy harvesting (EH) and discusses the techniques to optimize the conversion efficiency of the RF energy harvesting circuit under stringent conditions like arbitrary polarization, ultra low power (micro or nanopower) incidences and varying incident power densities. Harvested power management and application scenarios are also presented in this Chapter. Most of the design examples described are taken from the authors' recent publications.

The Chapter is organised as follows. Section 2.1 is the introduction on RF energy sources. Section 2.2 presents the antenna design for RF EH in the cellular band as well as DTV band. The key issue in RF energy harvesting is the RF-to-DC conversion efficiency and is discussed in Section 2.3, whereas Section 2.4 and 2.5 present the design of DTV and cellular energy harvesting rectifiers, respectively. The management of micropower levels of harvested energy is explained in Section 2.6. Performance analysis of the complete RF EH system is presented in Section 3.0. Finally, conclusions are drawn in Section 4.0.

1.1 RF energy sources

These include FM radio, Analogue TV (ATV), Digital TV (DTV), Cellular and Wi-Fi. We will present a survey of the measured E-field intensity (V/m) for some of these RF sources as shown in Table 1, [1]-[2]. Additionally, measured RF spectrums for DTV and Cellular signals are presented as shown in Fig. 1 to show on the potential for energy-harvesting in

these frequency bands. In general, many published papers on RF-to-DC conversion, have presented circuits capable of converting input or incident power as low as -20dBm. This means that, if an RF survey or scan finds signals in space, with power spectrum levels around -20dBm, then, it is potentially viable to harvest such signal power. In Fig. 1 (left side), the spectrum level is well above -20dBm and hence, a higher potential for energy harvesting. In Fig. 1 (right side), while the spectrum level is below -20dBm, what we observe is that the level increases with decrease in the distance toward the base station (BTS). Using free space propagation equation with this data, it was calculated that at a distance 1.4 m from the BTS, the spectrum level could measure 0dBm. An example calculation and plot for the estimated received power level, assuming 0dBi transmitter (BTS) and receiver antenna gains and free space propagation loss (FSPL) for FM and DTV is presented in Section 2.1.1. For the example estimation in Section 2.1.1, we select FM and DTV because they measured with a higher level than cellular and Wi-Fi for example.

Source	V/m	dBm	Reference	
FM radio	0.15~3		Asami et al.	
Analogue TV	0.3~2			
Digital TV	0.2~2.4	-40~0.0	Asami et al.	Arai et al.
Cellular		-65~0.0	Mikeka and Arai	
Wi-Fi		≅ -30		

Table 1. RF energy sources, measured data.

In Table 1, FM radio has the highest E-field intensity implying the highest potential for energy harvesting. However, due to the requirements for a large antenna size and the challenges for simulations and measurements at the FM frequency i.e. 100 MHz or less (See Section 2.2.3, example FM antenna at 80 MHz), this Chapter will focus on DTV (470~770 MHz band) and Cellular (2100 MHz band) energy harvesting.
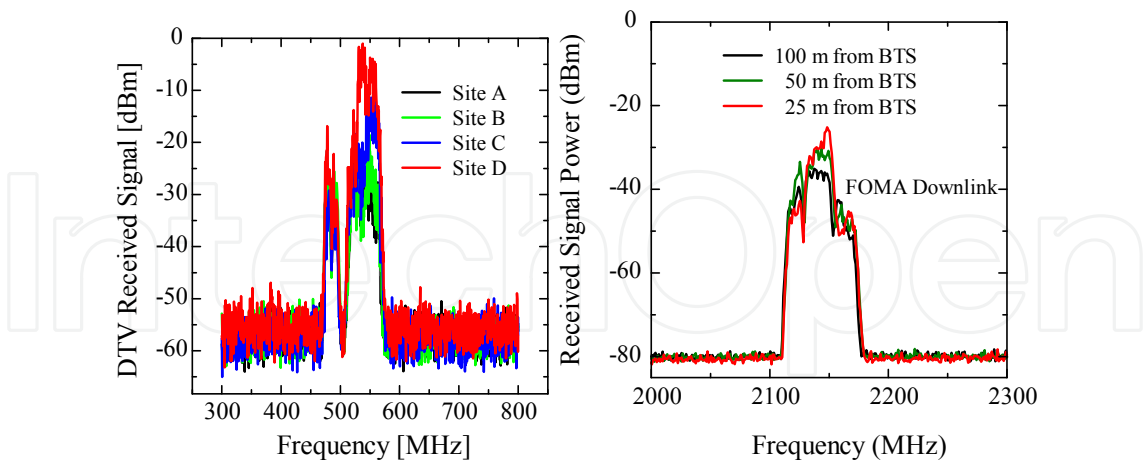

Fig. 1. DTV signal spectrum measured in Tokyo City (left side graph) and Cellular signal spectrum measured in Yokohama City (right side graph).

The received DTV signal power is high and also wide band, presenting high potential for increased energy harvesting unlike in cellular signals. We demonstrated in [2] that the total RF-to-DC converted power is roughly the integral over the DTV band (1), and is significantly larger than in the case of narrow band cellular energy harvesting.

$$P_{DC(DTV)} = \alpha \int_{470}^{770} \delta P_{DC}(f) df , \tag{1}$$

where α is the attenuation factor on the rectifying antenna's RF-to-DC conversion efficiency due to multiple incident signal excitation. δP_{DC} is the small converted DC power from each of the single DTV signals in the 470 MHz to 770 MHz band.

In detail, we derive (1) from fundamentals as follows.

The incident power density on the rectifying antenna (rectenna), $S(\theta, \phi, f, t)$, is a function of incident angles, and can vary over the DTV spectrum and in time. The effective area of the antenna, $A_{eff}(\theta, \phi, f)$, will be different at different frequencies, for different incident polarizations and incidence angles. The average RF power over a range of frequencies at any instant in time is given by:

$$P_{RF}(t) = \frac{1}{f_{high} - f_{low}} \int_{f_{low}}^{f_{high}} \int_{0}^{4\pi} S(\theta, \phi, f, t) A_{eff(\theta, \phi, f)} d\Omega df \tag{2}$$

The DC power for a single frequency (f_i) input RF power, is given by

$$P_{DC}(f_i) = P_{RF}(f_i, t) . \eta \left(P_{RF}(f_i, t), \rho, Z_{DC} \right) , \tag{3}$$

where η is the conversion efficiency, and depends on the impedance match $\rho(P_{RF}, f)$ between the antenna and the rectifier circuit, as well as the DC load impedance. The reflection coefficient in turn is a nonlinear function of power and frequency.

The estimated conversion efficiency is calculated by P_{RF}/P_{DC}. This process should be done at each frequency in the range of interest. However, DC powers obtained in that way cannot be simply added in order to find multi-frequency efficiency, since the process is nonlinear. Thus, if simultaneous multi-frequency or broadband operation like in DTV band is required, the above characterization needs to be performed with the actual incident power levels and spectral power density. In this Chapter, we shall demonstrate DTV spectrum power harvest, given a rectenna than has been characterised in house at each single frequency in the DTV band.

1.1.1 An example calculation and plot for the estimated received power level

In this example we consider Tokyo's DTV and FM base stations (BS) as the RF sources. Both DTV and FM BS transmitter power (P_t) equals 10 kW (70dBm). The antenna gains are assumed 0dBi in both cases but also at the points of reception for easiness of calculation but with implications as follows. Assuming 0dBi antenna at each reception point, demands that we specify the frequency of the transmitted signal. For this reason we specify DTV signal frequency to be equal to 550 MHz while the FM signal frequency equals 80 MHz (Tokyo FM).

The received power, P_r is calculated using the simplest form of Friis transmission equation given by

$$P_r = P_t + G_t + G_r + FSPL, \qquad (4)$$

where P_t = 70dBm, G_t = G_r = 0dBi. G_r is the receiving antenna gain while FSPL is the free-space path loss given by

$$FSPL(dB) = 20\log(d) + 20\log(f) + 32.45, \qquad (5)$$

where d is in (km) and f is in (MHz). The plot for the received power as a function of distance from the DTV and FM base stations is shown in Fig. 2.
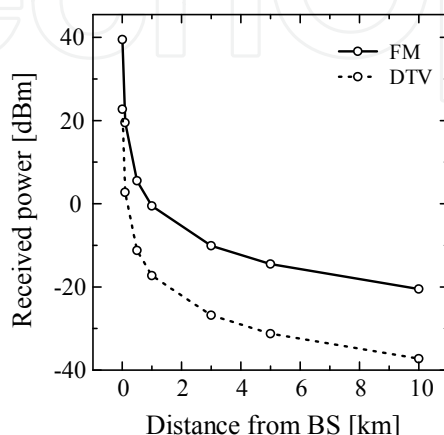

Fig. 2. DTV and FM received signal power level against distance.

With respect to Fig. 2, FM registers higher received power level than DTV at every reception point due to its lower transmit frequency and hence lower free-space path loss. For example at 1 km distance, FM received power level is -0.51dBm while for DTV, the received power is -17.26dBm. The important thing however, is that the received power level is frequency independent. It means that P_t is the transmitter power and the received power level at the position of distance d is $\dfrac{P_t}{4\pi d^2}$. However, if we assume 0dBi antenna at each reception point as in the above example, the power level is different because the antenna size of 0dBi is frequency dependent. As a result, high transmit power level is favorable for RF energy harvesting. Also near the base station is favorable.

1.2 Antenna design for the proposed RF energy harvesting (EH) system

It is well known that RF EH system requires the use of antenna as an efficient RF signal power receiving circuit, connected to an efficient rectifier for RF-to-DC power conversion. Depending on whether we want to harvest from cellular or DTV signals, the antenna design requirements are different. We will discuss the specific designs in the following sub sections.

1.2.1 Cellular energy harvesting antenna design

We propose a circular microstrip patch antenna (CMPA) for easy integration with the proposed rectifier (Section 2.5.1). However, the use of circular microstrip patch antennas (CMPA) is often challenged by the need for impedance matching, circular polarization (CP) and higher order harmonic suppression.

To address the above concerns, we create notches on the circular microstrip patch antenna. In our approach, we use only two, thin, fully parameterized triangular notches to achieve higher order harmonic suppression, impedance matching and circular polarization, all at once. This is the novelty in our proposed antenna. Our proposed CMPA is shown in Fig. 3. We study the behaviour of CMPA surface current vectors when notches (triangles ABC) are created on the structure at $\alpha = 45^0$ and $\alpha = 225^0$.
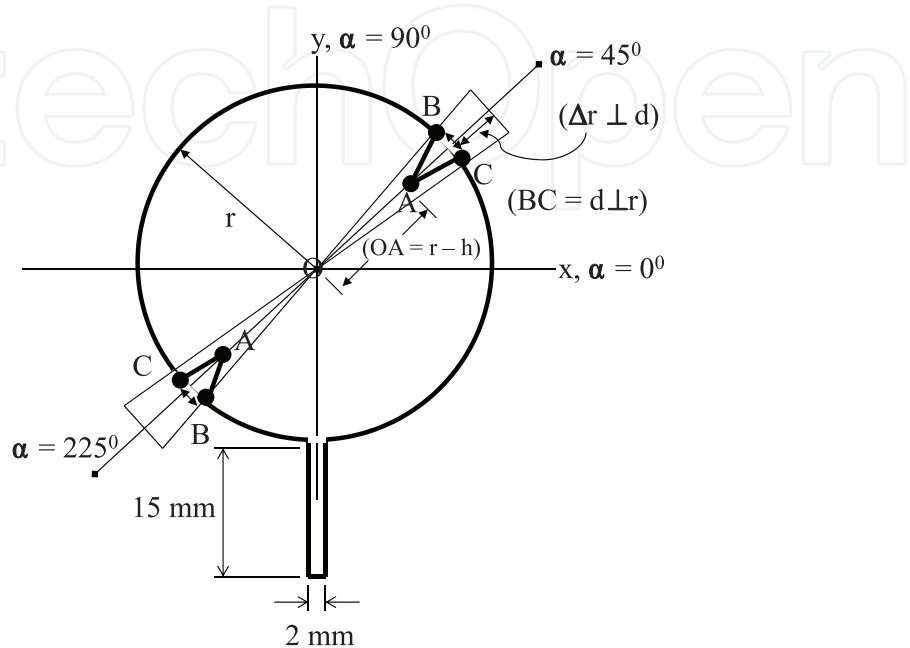

Fig. 3. Cellular energy harvesting antenna structure.

Notch parameters d and h in Fig. 3 were investigated by calculation using CST microwave Studio.

Without notches, the CMPA's input is not matched at f_c= 2.15 GHz as shown in Fig. 4 (left side). However, with notches, matching is achieved. The parameter combination d = 7 and h = 6 offers a matched and widest band input response and hence we adopt it for cellular energy harvesting applications.
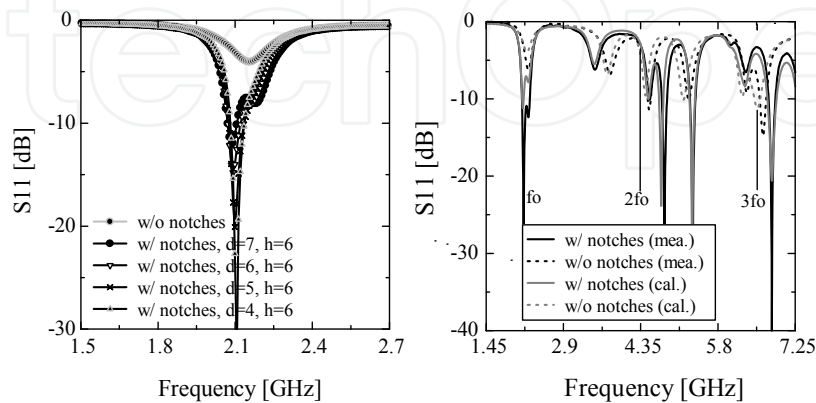

Fig. 4. *Left side: d* and *h* parameter investigation. *Right side:* Comparison between (cal.) and (mea.) S_{11} at f_0 = 2.175 GHz, $2f_0$ = 4.35 GHz and $3f_0$ = 6.53 GHz. The adopted notch parameters are *d*=7 mm while *h*= 6 mm.

The comparison between calculated and measured S_{11} is shown in Fig. 4 (right side). The 2nd and 3rd harmonics are suppressed as required by design. The comparison between calculated and measured radiation patterns is shown in Fig. 5, where $E_\vartheta \cong E_\varphi$ due to the 45⁰ tilted surface current vector. Ordinarily, without notches, the surface current vector is parallel to the microstrip feeder axis. In conclusion, our proposed CMPA is sufficiently able to suppress higher order harmonics while simultaneously radiating a circularly polarized (CP) wave. The CP is required to efficiently receive the arbitrary polarization of the incident cellular signals at the rectenna.
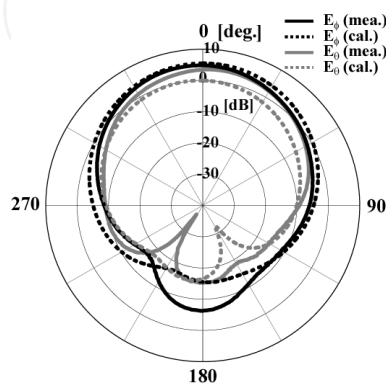
Fig. 5. Cellular energy harvesting antenna pattern at f_c= 2.15 GHz.

1.2.2 DTV energy harvesting antenna design

Unlike in the cellular energy harvesting antenna, the DTV energy harvesting antenna must be wideband (covering 470 MHz to 770 MHz), horizontally polarized and omni-directional.

The proposed antenna is typically a square patch (57 mm x 76 mm) with a partial ground plane (9 mm x 100 mm). The patch is indirectly fed by a strip line (9 mm x 3 mm). The proposed antenna geometry is shown in Fig. 6. The partial ground plane is used to achieve omni-directivity and a certain level of wide bandwidth. To tune the impedance of this antenna as well as to adjust the bandwidth within the target band, a "throttle" with stepped or graded structures is used between the microstrip feed line and the square patch, as shown in Fig. 6 (left side).
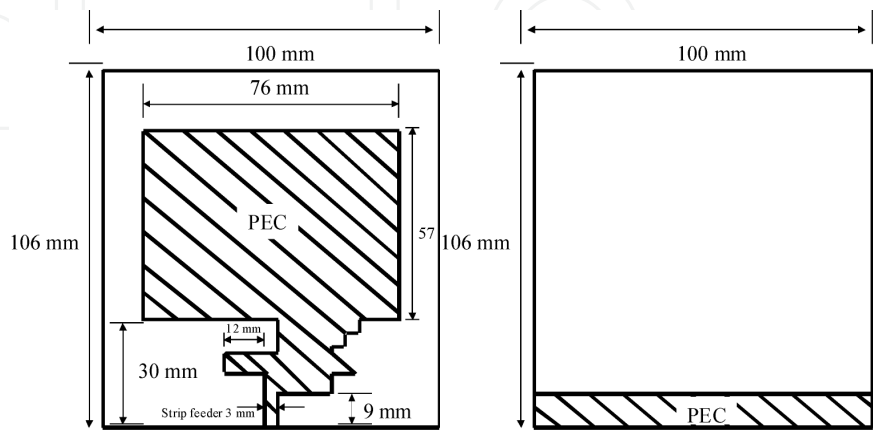

Fig. 6. Proposed DTV antenna geometry. *Left side:* Front view. *Right side:* Back view. The antenna is printed on FR4 substrate; t = 1.6 mm, ε_r = 4.4.

The input response for the proposed antenna is shown in Fig. 7 (left side). The omni directivity is confirmed by measurement at 500 MHz, 503 MHz, and 570 MHz as shown in Fig. 7 (right side). The radiation patterns shown in Fig. 7 are for the xz plane, which happens to be the vertical polarization for the antenna. DTV signals are horizontally polarized and therefore, when using this antenna, the orientation must be in such a way as to efficiently receive the DTV signal. Simply a 90 degree rotation of the antenna along the z axis achieves this requirement.
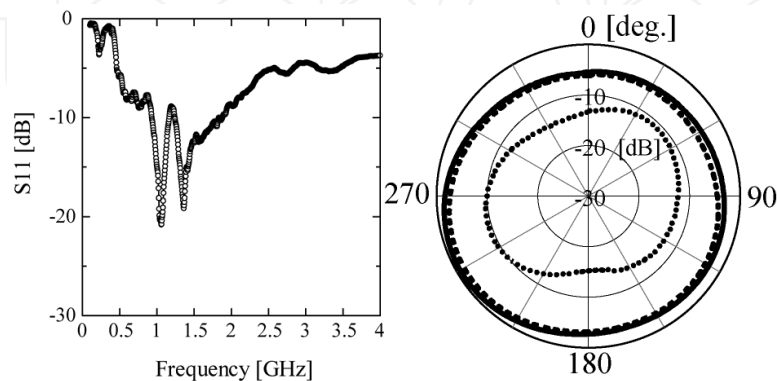
Fig. 7. Proposed DTV antenna performance. *Left side:* The antenna's measured input performance. *Right side:* The omni directivity in the vertical plane is confirmed at 500 MHz, 503 MHz, and 570 MHz. The outermost, black solid and dotted line patterns represent 503 MHz and 500 MHz directivity, respectively. The innermost dotted line pattern is the directivity at 570 MHz.

1.2.3 Example design for an 80 MHz FM half-wave dipole antenna

A half-wave dipole is the simplest practical antenna designed for picking up electromagnetic radiation signals, see Fig. 8 (courtesy of Highfields Amateur Radio Club). Calculating the optimal antenna length to pick up a certain frequency signal is fairly straightforward because antenna physics demand that the total length of wire used in the antenna be equal to one wavelength of the type of electromagnetic radiation it will be picking up. This means that the total length of the antenna should be equal to half the desired wavelength. By converting the 80 MHz frequency into a wavelength, you can thus obtain your antenna length as 1.875m by using the magic equation, $\lambda = \dfrac{c}{f}$. However, the actual length is typically about 95% of a half wavelength in free space, hence a half-wave dipole for this frequency should be 1.788m long, which would make each leg of the dipole 0.894m in length.

1.3 RF-to-DC conversion efficiency improvement techniques

A Schottky diode circuit connected to an antenna is used for RF-to-DC power conversion. To convert more of the antenna surface incident RF power to DC power, high RF-to-DC conversion efficiency is required of the rectifying circuit. Many authors have shown that the efficiency depends on several factors like Schottky diode type, harmonics suppression capability, load resistance selection, and the capability to handle arbitrary polarized incident waves. What is missing in most of these published works is the efficiency optimization for
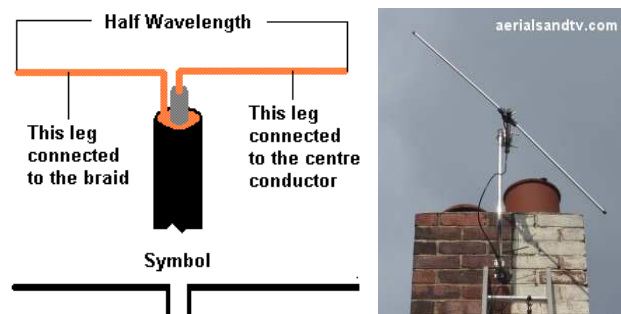
Fig. 8. Half-wave dipole. *Left side:* Antenna structure. *Right side:* Typical deployment.

ultra low power incident waves and the explanation of the physical phenomena behind most of the recommended efficiency optimization approaches.

This Chapter will show for example that a Schottky diode that delivers the highest efficiency at 0dBm incidence may not necessarily deliver the highest efficiency at lower power incidence e.g. –20dBm. We will therefore classify which diodes perform better at given power incidences; of course, this will also be compared to the diode manufacturers' application notes. Simulations in Agilent's ADS using SPICE and equivalent circuit models will compare the performance of few selected Schottky diodes namely; HSMS-2820, HSMS-2850, HSMS-2860, HSC-276A, and SMS7630. Moreover, the effect of the Schottky diode's junction capacitance (C_j) and junction bias resistance (R_j) on the conversion efficiency will be shown from which, special techniques for Schottky diode harmonic suppression and rectifying circuit loading for maximum efficiency point tracking will be presented.

1.3.1 The schottky diode

The classical *pn* junction diode commonly used at low frequencies has a relatively large junction capacitance that makes it unsuitable for high frequency application [3]. The Schottky barrier diode, however, relies on a semiconductor-metal junction that results in a much lower junction capacitance. This makes Schottky diodes suitable for higher frequency conversion applications like rectification (RF-to-DC conversion) [3]. We will demonstrate the effects of junction capacitance and resistance in the following sub section.

1.3.2 The effect of Schottky diode's C_j and R_j on the conversion efficiency

We have studied Schottky diode's C_j and R_j and published our results in [4]. In this work, we designed a rectifying antenna tuned for use at 2 GHz. The circuit proposed in [4] is a voltage doubler by configuration, but we replaced the amplitude detection diode (series diode) with its equivalent circuit adapted from [5]. The results of this investigation show that variation of C_j shifts the tuned frequency position and also introduces a mismatch in the resonant frequency, see Fig. 9 (left side graph). Therefore for this circuit at 2 GHz, we recommend using a Schottky diode having C_j = 0.2pF. In general, a smaller value of C_j is desirable at higher frequencies. Similarly, for R_j investigation, a smaller value is desirable for better matching at 2 GHz for example. If the R_j is increased towards 10kΩ, there is a mismatch in the resonant frequency but no shift in the frequency, see Fig. 9 (right side graph). Another approach to the study of Schottky diodes for higher frequency and efficiency rectenna design is presented in [6].
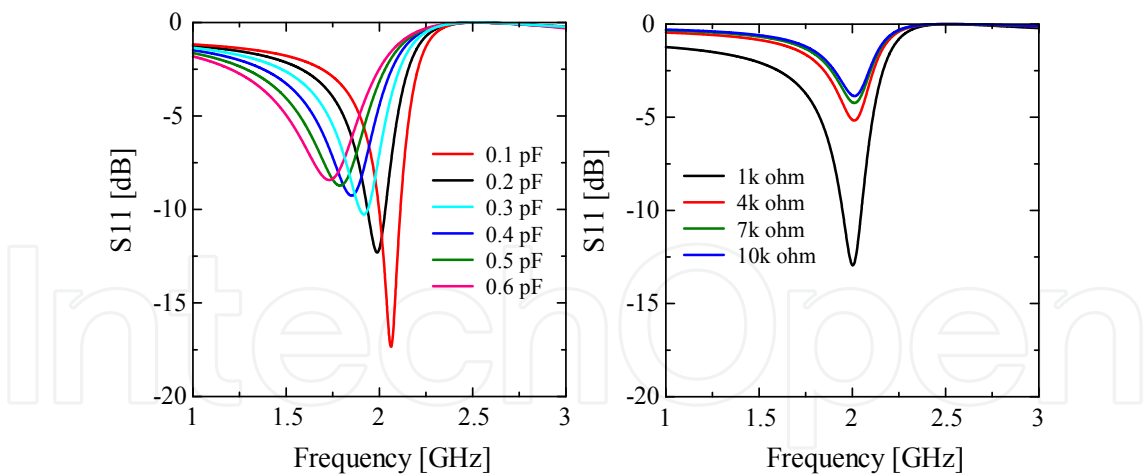
Fig. 9. Schottky diode's C_j effect (Left) and R_j effect (Right) on 2 GHz rectenna's input response.

1.4 Rectifying circuit for DTV energy harvesting

In the design of a DTV energy harvesting circuit, several basic design considerations must be paid attention to. First is the antenna; it must be wideband (covering 470 MHz to 770 MHz), horizontally polarized and omni-directional. Secondly is the rectifier; it must also be wideband, and optimized for RF-to-DC conversion for incident signal power at least -40dBm. Until recently, very few authors have published on DTV energy harvesting circuit. For the few publications, the antenna could not meet all those three requirements and a discussion on the performance of the harvesting circuit for ultra low power incidences has been neglected. In this Chapter we will present such a rectenna with conversion efficiencies above 0.4% at -40dBm, above 18.2% at -20dBm and over 50% at -5dBm signal power incidence. We will closely compare simulated and measured performance of the rectenna and discuss any observed disparities.

Agilent's ADS will be used to simulate the nonlinear behaviour of the rectifying circuit based on harmonic balance tuning methods. To simulate the multiple incident waves, a multi-tone excitation in the DTV band will be invoked. The wideband input characteristic will be achieved by the input matching inductors and capacitors.

The generic version of our proposed DTV energy harvesting circuit is shown below in Fig. 10. The implementation, however, is in two phases or scenarios as follows. First, we investigate the class called "ultra low power" DTV band rectenna. Secondly, we introduce the "medium power" DTV band rectenna.
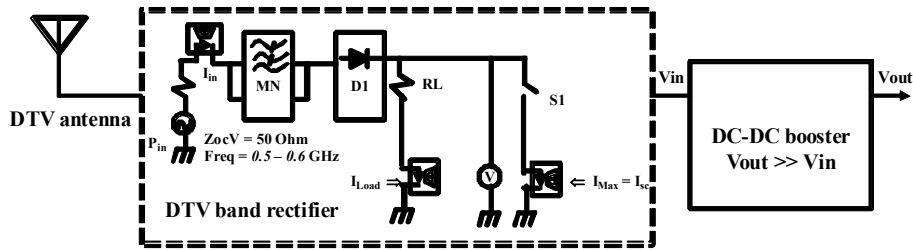

Fig. 10. Generic version of our proposed DTV energy harvesting circuit.

1.4.1 Ultra low power DTV rectenna

We define an ultra low power rectenna as one impinged by RF power incidence in the range between – 40dBm and -15dBm. Below in Fig. 11 is the circuit we designed; optimized for -20dBm input. The matching network is complex so as to achieve a wide band input characteristic. The fabricated circuit was well matched for the frequency range between 470 MHz and 600 MHz. More details about the circuit design can be found in [7].
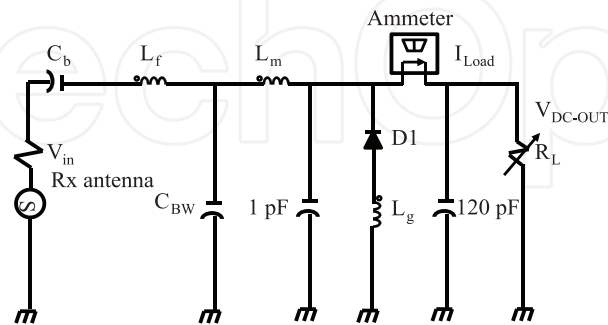
Fig. 11. Ultra low power DTV band rectenna circuit. SMS7630 Schottky diode by SKYWORKS offered the best performance.

The RF-to-DC conversion efficiency for this circuit is shown in Fig. 12 where at input power equal to -40dBm, efficiency is at least 0.4% and rectified voltage equals 1mV; at -20dBm, we have at least 18.2% by measurement and a rectified voltage of 61.7mV. The level of rectified voltage is too low and disqualifies this circuit for purposes of charging capacitors or batteries to accumulate such micropower over time. Instead, boosting the low voltage to usable levels is the option available and we shall discuss this at a later stage, (in Section 2.6).
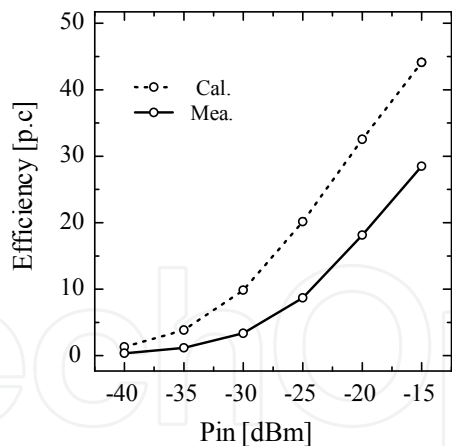
Fig. 12. Ultra low power DTV band rectenna efficiency.

1.4.2 Medium power DTV rectenna

We define a medium power rectenna as one impinged by RF power incidence in the range between – 5dBm and 0dBm. Below in Fig. 13 is the circuit we designed, optimized for -5dBm input. The matching network is simpler than as shown in section 2.4.1 since we require a narrow band around 550 MHz, with received peak power spectrum levels at least -5dBm. The circuit in Fig. 13 is a modification of Greinacher's doubler rectifier. In the circuit, C_b equals 1 pF and is used to block DC current against flowing towards the source. The shunt

capacitance, C_{BW} equals 3300 pF and is used to set the input bandwidth. The grounding inductance, L_g equals 56nH (optimal) and is used to improve the RF-to-DC conversion efficiency by cancelling the Schottky diodes (D_b and D_D) capacitive influence; thereby minimizing the harmonic levels (harmonic suppression). We used HSMS2850 diodes in these circuits for their better performance at this level of incident power.
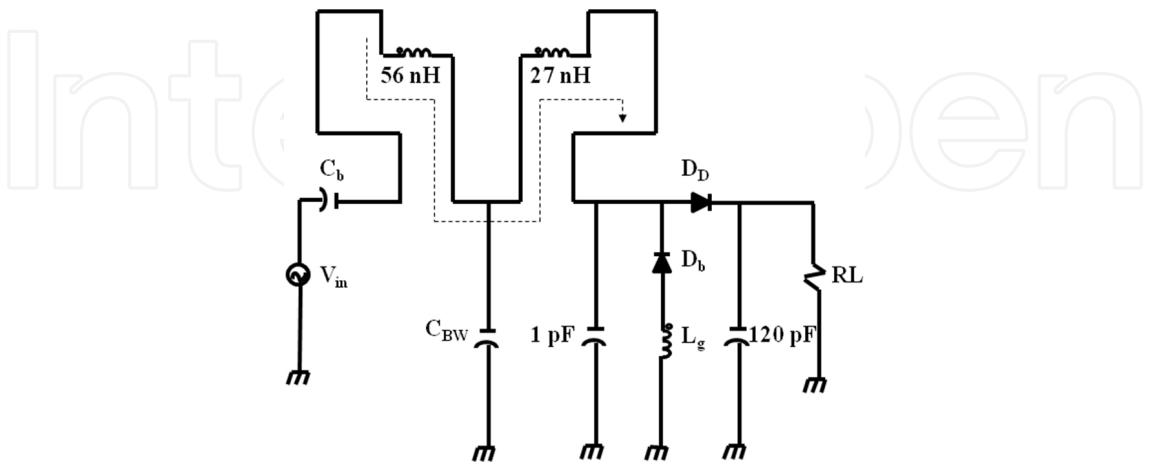

Fig. 13. Medium power DTV rectenna circuit. HSMS 2850 or 2820 from Hewlett-Packard offered the best performance.

The RF-to-DC conversion efficiency for this circuit is shown in Fig. 14 where at input power equal to -5dBm, we achieve at least 50% conversion efficiency by measurement, equivalent to 1.2 V DC rectified at 8.2kΩ optimal load. If we change the load to 47kΩ, over 2 V DC is rectified. This rectenna circuit is ideal for powering small sensors that run on 1.5 V or 2.2 V and draw around 6μA nominal current. If we need to power sensors demanding more power, say at least 2.2 V and 0.3mA to 1.47mA current consumption, we have to accumulate the power in a capacitor over time.
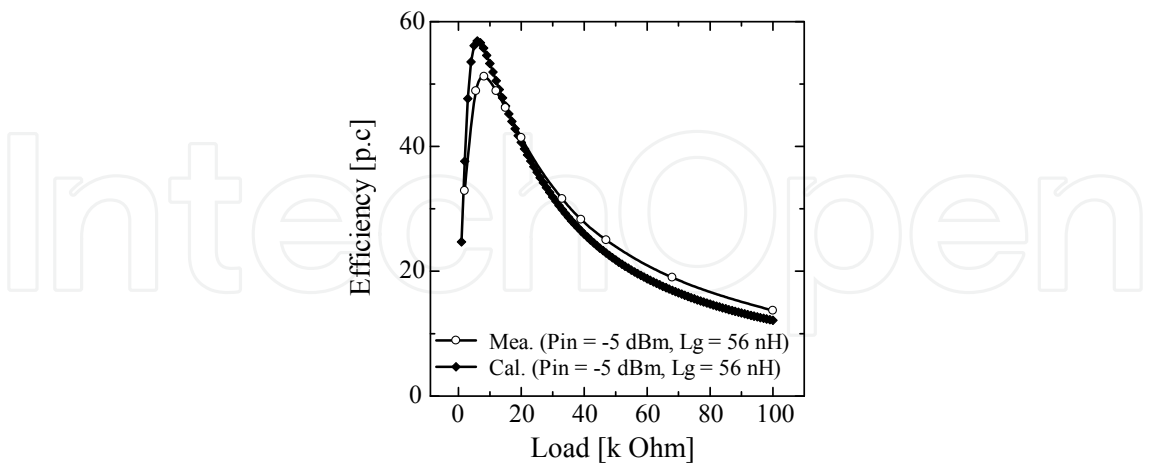

Fig. 14. Medium power DTV band rectenna efficiency.

1.4.3 DTV energy harvesting scenario and application demo

Using the medium power DTV band rectenna, connected to a gold capacitor as an accumulator, energy harvesting was initiated as shown in Fig. 15. Details about the gold

capacitor, which include its charge function, backup time and leakage losses are presented in [8]. For the scenario shown in Fig. 15, the accumulated voltage by measurement i.e. capacitor charge function follows the path;

$$V_{acc} = 0.5388\ln(t) + 1.4681 \tag{6}$$

where V_{acc} is the accumulated voltage in volts and t the time in hours. It takes 4.5 hours to accumulate 2.25 V, given a rectified charging voltage and current of 2.4 V and 51μA, respectively, supplied by the DTV band rectenna instantaneously.

With this rectenna, it was possible to power up many different kinds of sensors. Sensors with ultra low power consumption were powered directly, without need to accumulate the power in a capacitor, as shown in Fig. 16.

Fig. 15. DTV energy harvesting in a park at some line of sight from the base station.
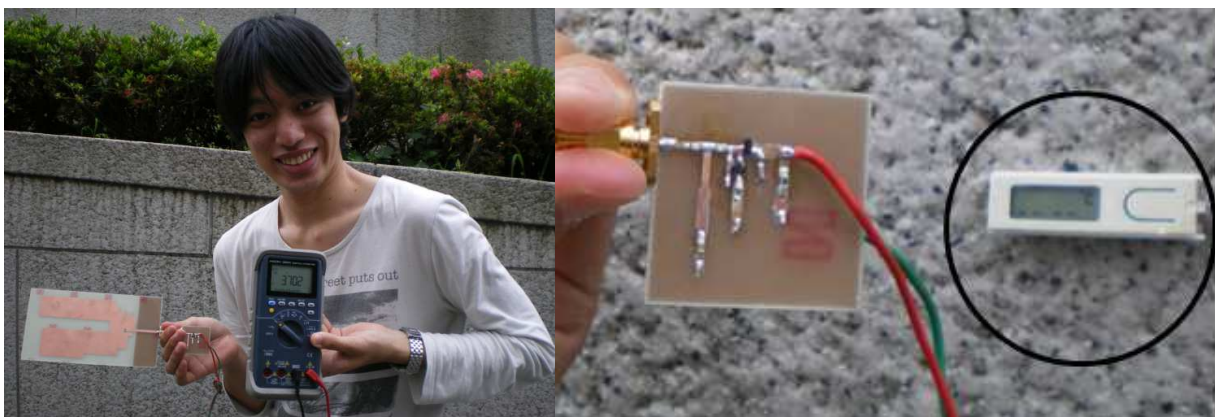
Fig. 16. Directly powering a thermometer mounted on a car park wall (right picture). The maximum instant voltage rectification on record equals 3.7 V (left picture).

1.5 Rectifying circuit for cellular energy harvesting

Unlike in the DTV energy harvesting circuit, for cellular energy harvesting, the antenna must be narrowband (50 MHz bandwidth is acceptable), and circularly polarized even

though cellular signals are vertically polarized. The circular polarization is desired to maximize the RF-to-DC conversion efficiency of the arbitrary polarization incident signals in the multipath environment. Similarly, the rectifier must be narrowband, and optimized for RF-to-DC conversion over a wide range of incident signal power.

Thinking about the potential applications for cellular energy harvesting is useful. Other authors have reported on powering a scientific calculator or a temperature sensor from GSM energy harvesting. In this Chapter we will present a special application for energy harvesting in the vicinity of the W-CDMA cellular base station and analyze the system performance by calculation from experimental data. A cellular energy harvesting circuit optimized for over 50% RF-to-DC conversion efficiency given approximately 0dBm incidence will be presented.

1.5.1 Cellular band rectenna

Below in Fig. 17 is the circuit we designed, optimized for 0dBm input. Simple input matching network is ideal since we require a narrow band response around 2.1 GHz. The optimum value for L_g equals 5.6nH, where L_g is used to improve the RF-to-DC conversion efficiency as earlier discussed. HSMS2850 diode was used.
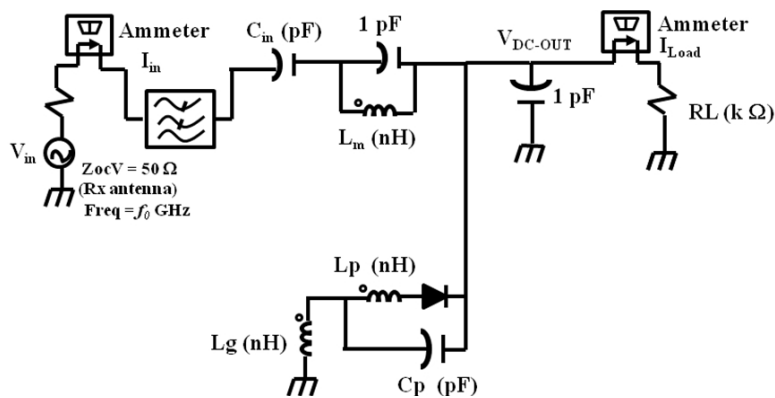

Fig. 17. Shunt rectifier configuration for the cellular band. The matching elements L_m = 3.2nH, while C_{in} =2.5pF. The load resistance is fixed at R_L = 2.1kΩ.
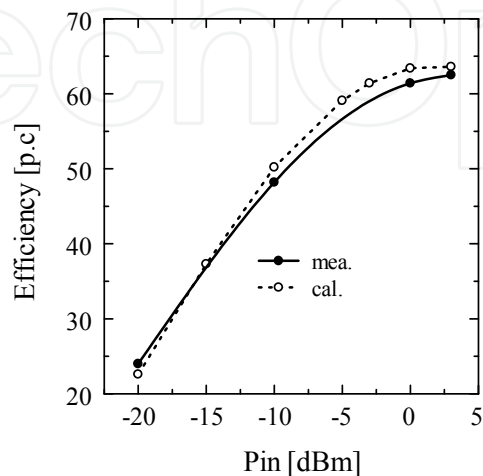

Fig. 18. Conversion efficiency as a function of input power (P_{in}) in the cellular band.

The RF-to-DC conversion efficiency for this circuit is shown in Fig. 18 where at input power equal to 0dBm, we achieve at least 60% conversion efficiency by measurement, given a 2.1kΩ optimal load. This rectenna circuit is ideal for powering small sensors that run on 1.5 V or 2.2 V and 6μA nominal current consumption. If we need to power sensors demanding more power, say at least 2.2 V and 0.3mA to 1.47mA, we have to accumulate the power in a capacitor over time as discussed in section 2.4.3 above.

1.5.2 Cellular energy harvesting application example

Environmental power generation in the neighbourhood of a cellular base station to power a temperature sensor is proposed as shown in Fig. 19 below. Electric field strength measurements in the base station neighbourhood have demonstrated the potential for environmental power generation, and the proposed temperature sensor system is designed based on these values. The rectenna described in Section 2.5.1 is used as the RF-to-DC rectifying circuit with the notched circular microstrip patch antenna (CMPA) proposed in Section 2.2.1. RF-to-DC conversion efficiency equal to 53.8% is obtained by measurement. The temperature sensor made for trial purposes clarifies the capability for temperature data wireless transmission for 20 seconds per every four hours in the base station neighbourhood.
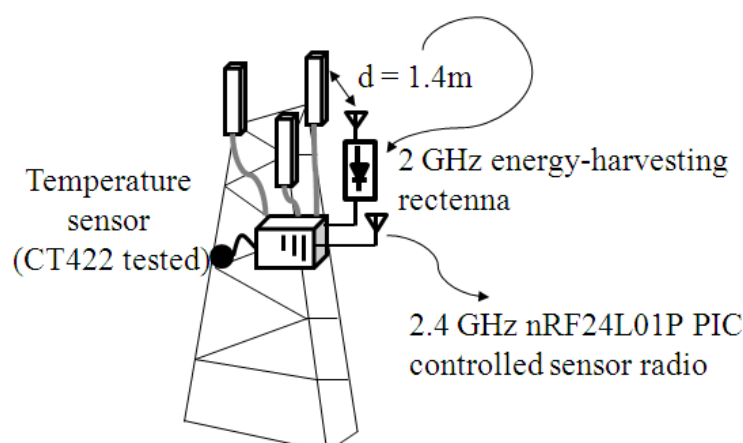

Fig. 19. Application example in the vicinity of the cellular base station.

1.6 Micropower energy harvesting management

A rectifying antenna circuit for -40dBm incident power harvesting generates 1mV at 2kΩ load, given 0.4% efficiency as presented in Section 2.4.1. At -20dBm incidence and at least 18.2% efficiency, 61.7mV is generated given a 2kΩ load [7]. The generated DC power in both of these two cases is in the μW range, hence the micropower definition. To manage such micropower, power accumulation or energy storage is required. Storage devices may either be a gold capacitor, super capacitor, thin film battery or the next generation flexible paper batteries. These storage devices have specific or standard maximum voltage and trickle charging current minimum requirements. Typically, gold capacitors have voltage ratings like 2.7 V, 5.5 V for 100 μA, 10mA or 100mA maximum discharge current. On the other hand, standard ratings for batteries are 1.8 V, 2 V, 3.3 V and 4.1 V. Therefore, to directly charge any of these storage devices from 1mV, or 61.7mV DC is impractical.

Published works have demonstrated the need for a DC-to-DC boost converter placed between the rectifying antenna circuit (rectenna) and the storage device. Recent efforts have demonstrated that a 40mV rectenna output DC voltage could be boosted to 4.1 V to trickle charge some battery. A Coilcraft transformer with turns ratio ($N_s : N_p$) equal to 100 was used in the boost converter circuit. An IC chip leading manufacturer (Linear Technology Corp., LT Journal, 2010) has released a linear DC-to-DC boost regulator IC chip capable of boosting an input DC voltage as low as 20 mV and supplying a number of possible outputs, specifically suited for energy harvesting applications. While this IC is a great milestone, readers and researchers need to understand the techniques to achieve such ICs and also the limitations that apply. In the following sub section, we will describe the methods toward designing a DC-DC boost converter, suitable for micropower RF energy harvesting.

In the design, we will attempt to clarify the parameters that affect the DC-DC conversion efficiency. For this design, Envelope simulation in Agilents's ADS is used. This simulation technique is the most efficient for the integrated rectenna and DC-DC boost converter circuits.

1.6.1 DC-DC boost converter design theory and operation

The DC-DC boost converter design theory and actual implementation are presented in this section. The inequality $V_{in} \ll V_{out}$ defines the boost operation. In this Chapter, our boost converter concept is illustrated in Fig. 20. A small voltage, V_{in} is presented at the input of the boost converter inductive pump which as a result, generates some output voltage, V_{out}. The output voltage is feedback to provide power for the oscillator. The oscillator generates a square wave, F_{OSC} that is used for gate signalling at the N-MOSFET switch.
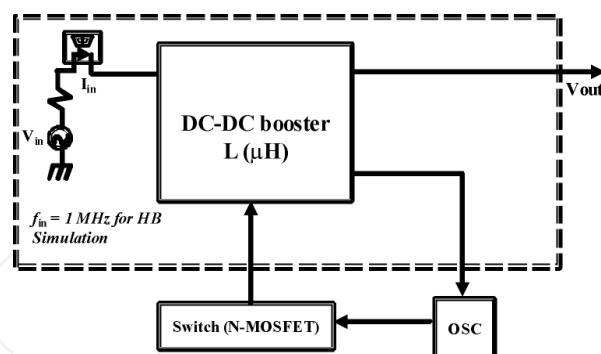

Fig. 20. Boost converter concept.

The drain signal of the N-MOSFET is used as the switch node voltage, V_{sn} at the anode of the diode inside the boost converter circuit block. From the concept presented in Fig. 20, the actual implemented circuit is shown in Fig. 21. The circuit was designed in Agilent's ADS and fabricated for investigation by measurement.

The circuit in Fig. 21 is proposed for investigation. Since a DC-DC boost converter is supposed to connect to the rectenna's output, it therefore, becomes the load to the rectenna circuit. This condition demands that the input impedance of the boost converter circuit emulates the known optimum load of the rectenna circuit. This has the benefit of ensuring

maximum power transfer and hence higher overall conversion efficiency from the rectenna input (RF power) to the boost converter output (DC power). In this investigation, as shown in [7], the optimum load for the rectenna is around 2kΩ. In general, emulation resistance R_{em} is given by
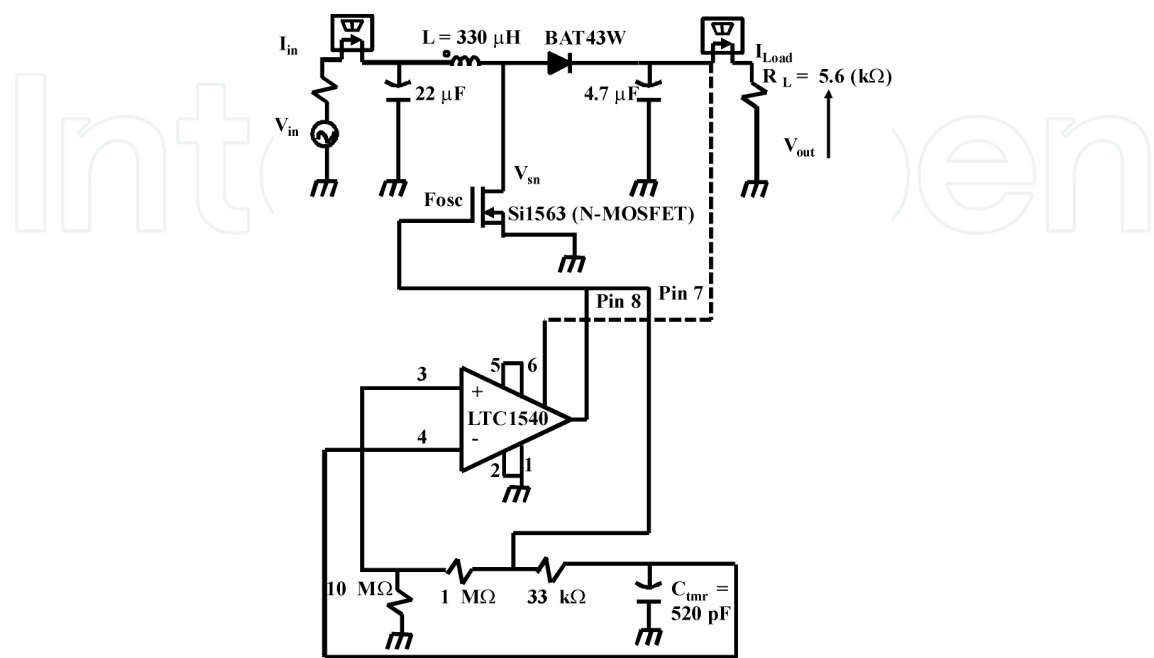

Fig. 21. The proposed boost converter circuit diagram. Designed in Agilent's ADS and fabricated for investigation by measurement.

$$R_{em} = \frac{2LT}{t_1^2 k}\left(\frac{M-1}{M}\right) \tag{7}$$

where L is the inductance equal to 330μH as shown in Fig. 20, $M = \frac{V_{out}}{V_{in}}$, T is the period of F_{OSC}, t_1 is the switch"ON" time for the N-MOSFET, and k is a constant that according to [3] is a low frequency pulse duty cycle if the boost converter is run in a pulsed mode and typically, k may assume values like 0.06 or 0.0483. With reference to (7), we select L as the key parameter for higher conversion efficiency while V_{in} = 0.4 V DC is selected as the lowest start up voltage to achieve oscillations and boost operation. Computing the DC-DC boost conversion efficiency against different values of L, we have results as shown in Fig. 22.

From the results above, L = 100μH is the optimum boost inductance that ensures at least 16.5% DC-DC conversion efficiency, given R_L = 5.6kΩ.

Now having selected the optimum boost inductance given some load resistance, the emulation resistance shown in Fig. 23 is evaluated from the ratio of voltage versus current at the boost converter circuit's input.

The results show a constant resistance value against varying inductance. In general, we can say that this boost converter circuit has a constant low input impedance around 82.5Ω. This impedance is too small to match with the optimum rectenna load at 2kΩ. This directly affects the overall RF-to-DC conversion efficiency.
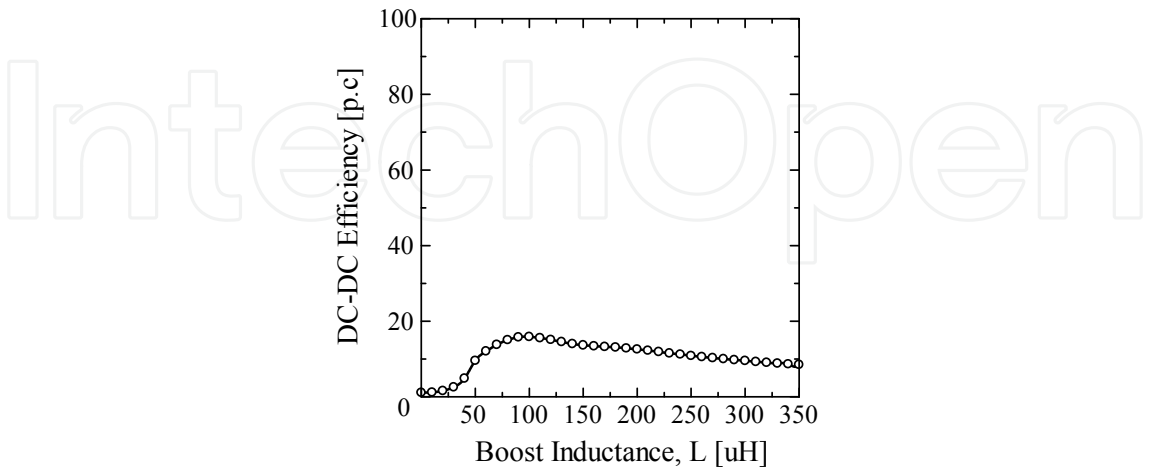
The results show a constant resistance value against varying inductance. In general, we can say that this boost converter circuit has a constant low input impedance around 82.5Ω. This impedance is too small to match with the optimum rectenna load at 2kΩ. This directly affects the overall RF-to-DC conversion efficiency.

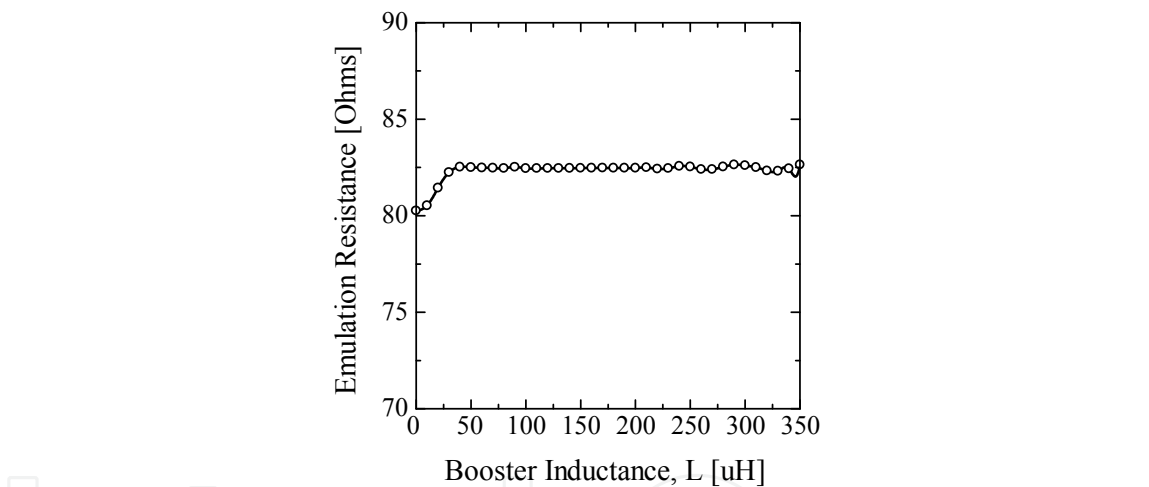Fig. 22. Boost inductance variation with DC-DC conversion efficiency for a 5.6 kΩ load.

Fig. 23. Boost converter's input impedance: the emulation resistance.

Another factor, which affects the overall conversion efficiency is the power lost in the oscillator circuit. Unlike the circuit proposed in [9], which uses two oscillators; a low frequency (LF) and high frequency (HF) oscillator; in Fig. 21, we have attempted to use a single oscillator based on the LTC1540 comparator, externally biased as an astable multivibrator.

The power loss in this oscillator is the difference in the DC power measured at Pin 7 (supply) to the power measured at pin 8 (output). We term this loss, L_{osc}; converted to heat or sinks through the 10MΩ load. A comparison of the oscillator power loss to the power available at the boost converter output is shown in Fig. 24.

Looking at Fig. 24; we notice that the power loss depends on whether the oscillator output is high or low. The low loss corresponds to the quiescent period where the power lost is

almost negligible. However, during the active state, the lost power (power consumed by the oscillator) nearly approaches the DC power available at the boost converter output. This results in low operational efficiency.
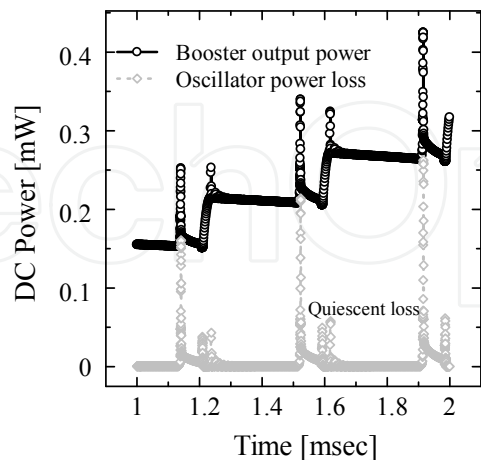

Fig. 24. The power loss in the oscillator.

To confirm whether or not the circuit of Fig. 21 works well, we did some measurements and compared them with the calculated results. Unlike in calculation (simulation), during measurement, L = 330μH was used due to availability. All the other component values remain the same both in calculation and measurement. In Fig. 25 (left side graph) and (right side graph), we see in general that the input voltage is boosted and also that the patterns of F_{osc} and V_{sn} are comparable both by simulation and measurement. To control the duty cycle of the oscillator output (F_{osc}), and the level of ripples in the boost converter output voltage (V_{out}), we change the value of the timing capacitance, C_{tmr} in the circuit of Fig. 21. Simulations in Fig. 25 (left side graph) show that $C_{tmr} = 520$pF realizes a better performance i.e. nearly constant V_{out} level (very low ripple).
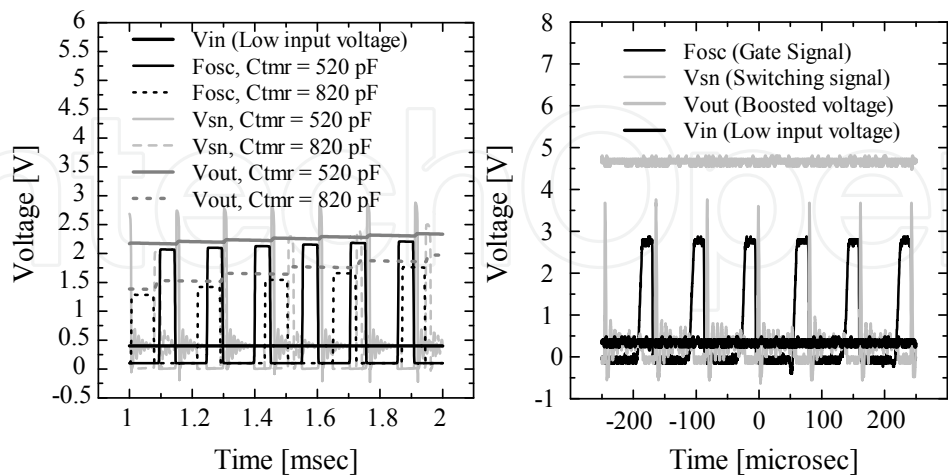

Fig. 25. Voltage characteristics of the developed boost converter circuit. The left side graph represents simulation while the right side graph is for measurements.

Generally, we observe that with this kind of boost converter circuit topology, it is difficult to start up for voltages as low as 61.7mV DC generated by the rectenna at -20dBm power

incidence and at least 18.2% rectenna RF-to-DC conversion efficiency. Self starting is the issue for this topology at very low voltages.

At least 11.3% DC-DC conversion efficiency was recorded by measurement and is comparable to the calculation in Fig. 22. During measurement it was clearly revealed that the boost converter efficiency does depend on the value of **L** and the duty cycle derived from **t₁**. To efficiently simulate the complete circuit, from the RF input to the DC output, envelope transient simulation (ENV) in Agilent's ADS was used. The (ENV) tool is much more computationally efficient than transient simulation (Tran). This simulation is appropriate for the boost converter circuit's resistor emulation task. Moreover, the boost converter's DC-DC conversion efficiency, and the overall RF-to-DC conversion efficiency can be calculated at once with a single envelope transient simulation.

In summary, though not capable to operate for voltages as low as 61.7mV DC, the proposed boost converter has by simulation and measurement demonstrated the capability to boost voltages as low as 400mV DC, sufficient for battery or capacitor recharging, assuming that the battery or the capacitor has some initial charge or energy enough to provide start-up to the boost converter circuit.

The limitations of our proposed boost converter circuit include; low efficiency, lack of self starting at ultra low input voltages, and unregulated output. To address these limitations, circuit optimization is required. Moreover, alternative approaches which employ a flyback transformer to replace the boost converter inductance must be investigated. A regulator circuit with Low Drop Out (LDO) is necessary to fix the boost converter output voltage commensurate with standard values like 2.2 V DC for example. For further reading, see [7]

2. Performance analysis of the complete RF energy harvesting sensor system

To demonstrate how one may analyze the performance of an RF energy harvesting system including its application, we extend the discussion of Section 2.5.2 to this Section. We propose a transmitter assembled as in Fig. 26 for temperature sensor wireless data transmission.
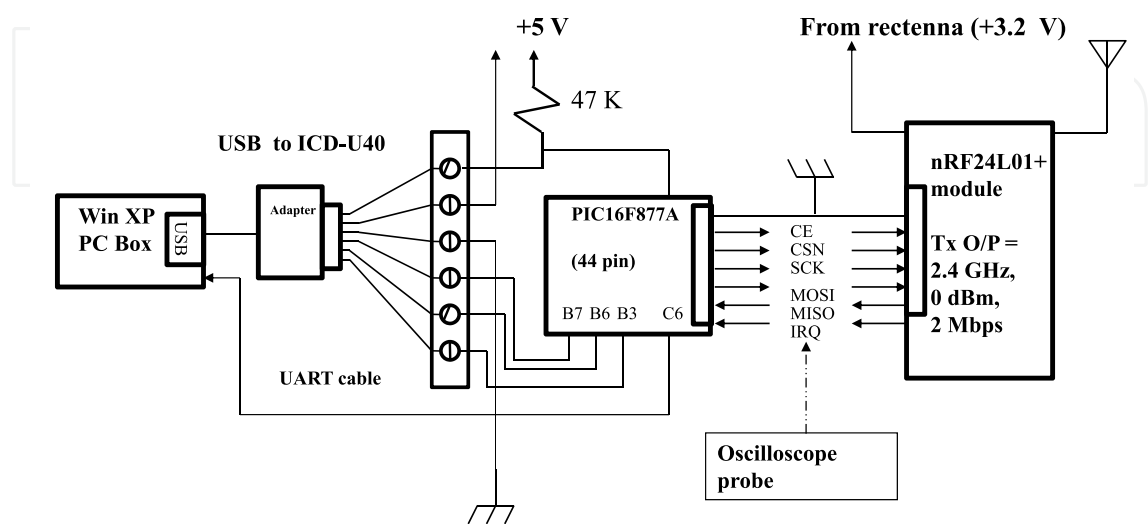

Fig. 26. The assembly and test platform for the proposed battery-free sensor transmitter.

The transmitter consists of one-chip microcomputer (MCU) PIC16F877A and wireless module nRF24L01P for the control, and MCU can be connected with an outside personal computer using ICD-U40 or RS232 cable. The wireless module operates in transmission and reception mode, and controls power supply on-off, transmitting power level, the receiving mode status, and transmission data rate via Serial Peripheral Interface (SPI). Figure 27 shows the operation flow when transmitting.
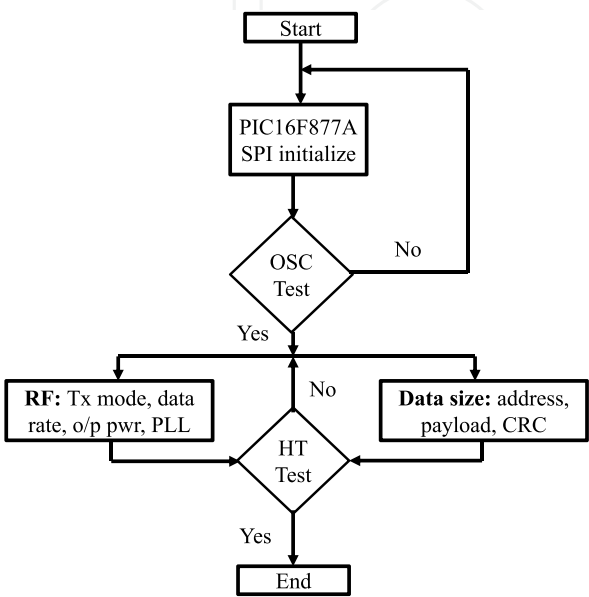

Fig. 27. Operation flow during transmission.

The experimental system composition is shown in Fig. 28 to transmit acquired data by the temperature sensor with WLAN at 2.4 GHz (ISM band). An ISM band sleeve antenna is used for the transmission. Using the cellular band rectenna shown and discussed in Section 2.5.1, at least 3.14 V is stored in the electric double layer capacitor over a period of four hours. To harvest a maximum usable power for the overall system, we charge the capacitor up to 5V. The operation voltage for the wireless module presented in Fig. 26 above is between 1.9V and 3.6V.

The signal was transmitted from the wireless module while a sleeve antenna, same like the one for transmission was used with the spectrum analyzer and the reception experiment was performed. Received signal level equal to -43.4dBm was obtained at a distance 3.5m between transmitter and reception point. The capacitor's stored voltage was used to supply the wireless module in the above-mentioned experiment. Successful transmission was possible for 5.5 minutes after which, the capacitor terminal voltage decreased from 3.16V to 1.47V, and the transmission ended. The sending and receiving distance of data can be estimated to be about 10m when the sensitivity of the receiver is assumed to be -60dBm, given 0dBm maximum transmit power.

Hereafter, the overall system examination is done by environmental power generation using the transmitted electric waves from the cellular phone base station, proposed based on the above-mentioned results. First of all, the power consumption shown in Fig. 29 is based on the fact that 120mW (5V, 24mA) is saved in the electric double layer capacitor by environmental power generation, achieved by calculation as discussed earlier.
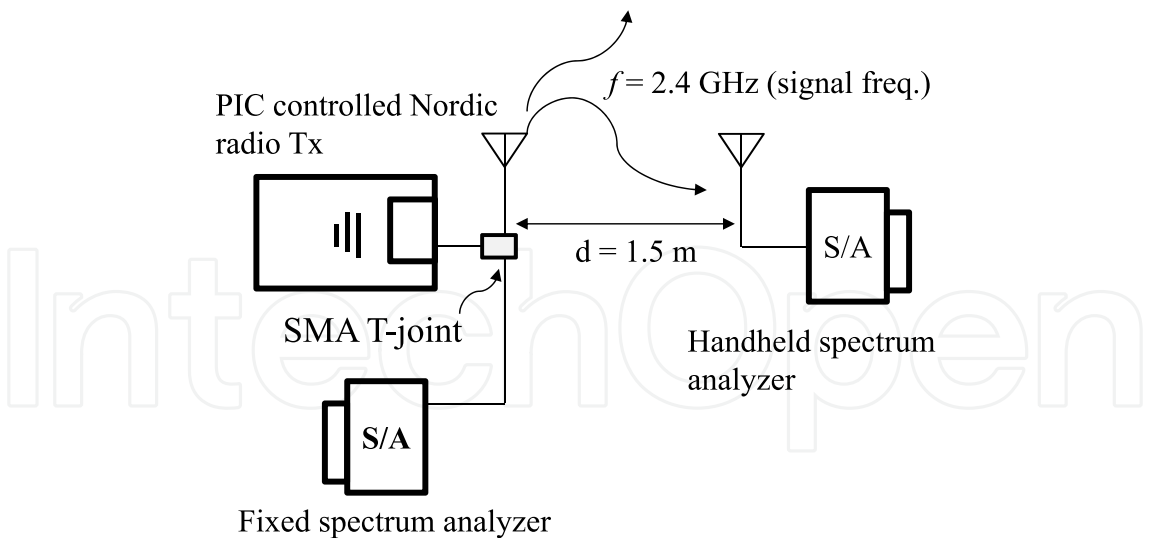
Fig. 28. Indoor measurement setup for received traffic from the sensor radio transmitter.
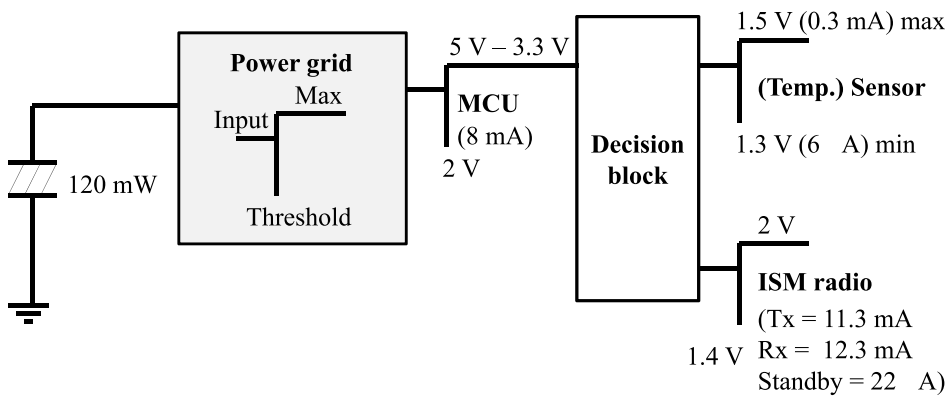

Fig. 29. Power management scheme for the cellular energy-harvesting sensor node.

The sensor data packet is transmitted wirelessly in ShockBurst mode for energy efficient communication. The data packet format includes a pre-amble (1 byte), address (3 bytes), and the payload i.e. temperature data (1 byte). The flag bit is disregarded for easiness, and cyclic redundancy check (CRC) is not used.

The operation of the proposed system is provisionally calculated. When the rectenna is set up in the place where power incidence of 0dBm is obtained in the base station neighbourhood (as depicted in Section 2.5.2), an initially discharged capacitor accumulates up to 3.3V by a rectenna with 53.8% conversion efficiency (presented in Section 2.5.1). At this point, it takes 1.5 minutes to start and to initialize a wireless module, and the voltage of the capacitor decreases to 2V. This trial calculation method depends on the capacitor's back up time discussed in [8]. After this, when the wireless module is assumed to be in sleep mode, the capacitor is charged by a 0.28mA charging current for four hours whereby the capacitor's stored voltage increases up to 5V. The power consumption in the sleep mode or standby is 33µW (1.5V, 22µA).

When the wireless module starts, after data transmission and the confirmation signal is sent, the voltage of the capacitor decreases by 0.6V, and consumes the electric power of 7.4mW.

The voltage of the capacitor decreases to 2V when 3.2mW is consumed to the acquisition of the sensor data, and the operation time of MCU is assumed to be one minute to the data storage in the wireless module etc. As for the capacitor voltage, when the wireless module continuously transmits data for 20 seconds, it decreases from 2V to 1.4V and even the following operation saves the electric power. Therefore, a temperature sensing system capable of transmitting wireless data in every four hours becomes feasible by environmental power generation from the cellular phone base station if we consider intermittent operation by sleep mode.

3. Conclusion

This Chapter has given an overview of the present energy harvesting sources, but the focus has stayed on RF energy sources and future directions for research. Design issues in RF energy harvesting have been discussed, which include low conversion efficiency and sometimes low rectified power. Solutions have been suggested by calculation and validated by measurement where possible, while highlighting the limitations of the proposed solutions. Potential applications for both DTV and cellular RF energy harvesting have been proposed and demonstrated with simple examples. A discussion is also presented on the typical performance analysis for the proposed RF energy harvesting system with sensor application.

4. Acknowledgment

5. References

[1] Keisuke, T.; Kawahara, Y. & Asami, T. (2009). *RF Energy Intensity Survey in Tokyo..,* (c)2009 IEICE, B-20-3, Matsuyama-shi, Japan

[2] Mikeka, C.; Arai, H. (2011). *Dual-Band RF Energy-Harvesting Circuit for Range Enhancement in Passive Tags,* (c)2011 EuCAP, Rome, Italy

[3] Pozar, D. (2005). *Microwave Engineering,* Wiley, ISBN 978-0-471-44878-5, Amherst, MA, USA

[4] Mikeka, C.; Arai, H. (2010). Techniques for the Development of a Highly Efficient Rectenna for the Next Generation Batteryless System Applications, *IEICE Tech. Rep.,* pp. 101-106, Kyoto, Japan, March, 2010

[5] http://www.secomtel.com/UpFilesPDF/PDF/Agilent/PDF_DOCS/SKYDIODE/ 03_SKYDI/HSMS2850.PDF (Last accessed on 13 July, 2011)

[6] McSpadden, J. et al., H. (1992). Theoretical and Experimental Investigation of a Rectenna Element for Microwave Power Transmission, *IEEE Trans., on Microwave Theory and Tech., Vol. 40, No. 12.,* pp. 2359-2366, Dec., 1992

[7] Mikeka, C.; Arai, H. ; Georgiadis A. ; and Collado A. (2011). DTV Band Micropower RF Energy-Harvesting Circuit Architecture and Performance Analysis, *RFID-TA Digest,* Sitges, Spain, Sept., 2011

[8] Mikeka, C.; Arai, H. (2009). Design of a Cellular Energy-Harvesting Radio, *Proc. 2 nd European Wireless Technology Conf.,* pp. 73-76, Rome, Italy, Sept., 2009

[9] Popovic Z., et al., (2008). Resistor Emulation Approach to Low-Power RF Energy Harvesting, *IEEE Trans. Power Electronics, Vol. 23, No. 3,* 2008
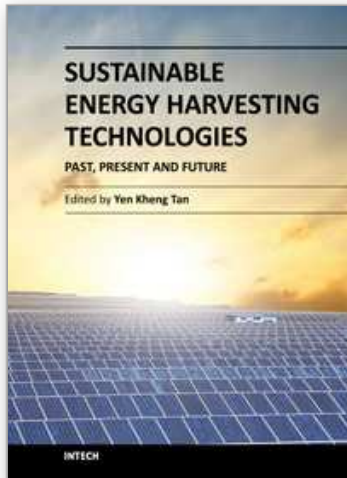
Sustainable Energy Harvesting Technologies - Past, Present and Future
Edited by Dr. Yen Kheng Tan

In the early 21st century, research and development of sustainable energy harvesting (EH) technologies have started. Since then, many EH technologies have evolved, advanced and even been successfully developed into hardware prototypes for sustaining the operational lifetime of low?power electronic devices like mobile gadgets, smart wireless sensor networks, etc. Energy harvesting is a technology that harvests freely available renewable energy from the ambient environment to recharge or put used energy back into the energy storage devices without the hassle of disrupting or even discontinuing the normal operation of the specific application. With the prior knowledge and experience developed over a decade ago, progress of sustainable EH technologies research is still intact and ongoing. EH technologies are starting to mature and strong synergies are formulating with dedicate application areas. To move forward, now would be a good time to setup a review and brainstorm session to evaluate the past, investigate and think through the present and understand and plan for the future sustainable energy harvesting technologies.

How to reference
In order to correctly reference this scholarly work, feel free to copy and paste the following:

Chomora Mikeka and Hiroyuki Arai (2011). Design Issues in Radio Frequency Energy Harvesting System, Sustainable Energy Harvesting Technologies - Past, Present and Future, Dr. Yen Kheng Tan (Ed.), ISBN: 978-953-307-438-2, InTech, Available from: http://www.intechopen.com/books/sustainable-energy-harvesting-technologies-past-present-and-future/design-issues-in-radio-frequency-energy-harvesting-system

INTECH
open science | open minds